SIAM J. NUMER. ANAL.
Vol. 27, No. 5, pp. 1187-1196, October 1990

004

A TRIANGULATION ALGORITHM FOR FAST ELLIPTIC SOLVERS BASED ON DOMAIN IMBEDDING*

CHRISTOPH BÖRGERS†

Abstract. The following triangulation problem is considered. Let R be a rectangle, and Ω an open domain whose closure is contained in R. Consider a rectangular grid covering R. Perturb this grid by shifting points close to the boundary $\partial\Omega$ onto $\partial\Omega$. This results in a quadrilateral, almost rectangular grid. Divide each cell of this grid into two triangles along one of its diagonals. This results in a triangulation of R. A subset of this triangulation is a triangulation of an approximation Ω^h to Ω. The distance between $\partial\Omega^h$ and $\partial\Omega$ is required to be $O(h^2)$, where h denotes the maximum meshwidth of the rectangular grid. All triangles should be nondegenerate.

Triangulations of this kind are needed for finite element domain imbedding methods for elliptic boundary value problems. A particularly simple example of such a method is reviewed. The convergence theory for this method motivates our definition of nondegeneracy of triangles.

For $\partial\Omega \in C^2$, an algorithm for constructing triangulations with the desired properties is described. If the boundary has corners, the condition that the distance between $\partial\Omega^h$ and $\partial\Omega$ be $O(h^2)$ cannot always be satisfied. However, domains with corners are also discussed, and a modification of the algorithm for this case is described.

Key words. triangulation, fast elliptic solvers

AMS(MOS) subject classifications. 65N50, 65N20

1. Introduction. Domain imbedding methods are special solution techniques for the large linear systems of equations arising in the discretization of linear elliptic boundary value problems. The principle is to solve a boundary value problem on a domain Ω using auxiliary boundary value problems on a rectangle R containing Ω. The motivation is that elliptic solvers on rectangles are more convenient, and sometimes more efficient, than elliptic solvers on general domains. A review of some of the literature on domain imbedding methods can be found in [1].

Finite element domain imbedding methods require special triangulations; see [4], where an algorithm for generating such triangulations is proposed. In the present paper, we describe an alternative algorithm for this task, more general than that of [4].

We give an outline of our algorithm. Consider a rectangular grid $\hat{\Gamma}$ covering R. Denote the gridpoints by

$$\hat{\mathbf{x}}_{ij} = (\hat{x}_i, \hat{y}_j), \quad 0 \leqq i \leqq I, \quad 0 \leqq j \leqq J. \tag{1}$$

Perturb this grid by moving points near the boundary $\partial\Omega$ onto $\partial\Omega$. This results in a quadrilateral, almost rectangular grid Γ, whose points we denote by

$$\mathbf{x}_{ij} = (x_{ij}, y_{ij}), \quad 0 \leqq i \leqq I, \quad 0 \leqq j \leqq J. \tag{2}$$

There is a natural one-to-one correspondence between the points in $\hat{\Gamma}$ and those in Γ; compare Figs. 1 and 2 in § 4 below. Divide each of the cells of the perturbed grid Γ into two triangles along one of its diagonals. This results in a triangulation $(\tau_\nu)_{1 \leqq \nu \leqq n}$

* Received by the editors April 19, 1989; accepted for publication (in revised form) September 22, 1989. This work was supported in part by the Applied Mathematical Sciences Subprogram of the Office of Energy Research under contract DE-AC03-76SF00098 at the Lawrence Berkeley Laboratory, and in part by National Science Foundation grant NSF-DMS-8801991. The manuscript was completed while the author was a visiting Scientist at the IBM Thomas J. Watson Research Center.

† Department of Mathematics, University of Michigan, Ann Arbor, Michigan 48109.

of R, with $n=2I^2J^2$. The details of this procedure are such that all triangles are nondegenerate, in the sense that no small angles occur. (A slightly different but roughly equivalent definition of "nondegeneracy," motivated by the convergence theory of domain imbedding methods, is used in § 3.)

Some of the triangles form a triangulation of an approximation Ω^h to Ω:

$$\Omega^h = \bigcup_{\nu=1}^{k} \tau_\nu. \tag{3}$$

If $\partial\Omega \in C^2$, the distance between $\partial\Omega^h$ and $\partial\Omega$ is $O(h^2)$, where h denotes the maximum meshwidth of the rectangular grid.

We remark that the algorithm proposed in [4] may lead to degenerate triangles, even if $\partial\Omega$ is smooth. The reason will be pointed out in § 3.

In § 2, we give a brief description of a simple finite element domain imbedding method, for the purpose of motivation. In § 3, we describe and study our triangulation algorithm in detail. For illustration, we show plots of triangulations generated by our algorithm in § 4.

A Fortran code implementing the algorithm is available from the author. This code was used in performing the numerical experiments on domain imbedding methods reported in [1].

2. Domain imbedding for Neumann problems. For the purpose of motivation, we shall review a particularly simple domain imbedding algorithm in this section. This algorithm was proposed and studied in [4]. However, our description follows [1] and differs from that given in [4]. In addition to reviewing the domain imbedding algorithm and its convergence theory, we will give an estimate (Theorem 2) that is central for the motivation of our triangulation algorithm.

Let Ω be a bounded domain in the plane. Consider a Neumann problem of the form

$$-\triangle\phi = f \quad \text{in } \Omega, \tag{4}$$

$$\frac{\partial\phi}{\partial n} = g \quad \text{on } \partial\Omega \tag{5}$$

($\partial/\partial n$ denotes the exterior normal derivative).

We discretize this problem using piecewise linear Lagrangian finite elements based on the triangulation $(\tau_\nu)_{\nu=1,\cdots,k}$ of Ω^h. We will also use auxiliary boundary value problems on the entire rectangle R, with Neumann boundary conditions on ∂R. The finite element discretization of these problems, based on the triangulation $(\tau_\nu)_{\nu=1,\cdots,n}$ of R, results in a system of linear equations

$$K\mathbf{x} = \mathbf{r}, \tag{6}$$

where K is the stiffness matrix. The entries in K are of the form

$$\int_R \nabla\phi_i^T \cdot \nabla\phi_j \, d\mathbf{x} \tag{7}$$

where ϕ_i and ϕ_j are canonical basis functions of the finite element space, i.e., the space of continuous functions on R that are linear on each triangle τ_ν.

We order the unknowns such that K takes the form

$$K = \begin{pmatrix} K_{11} & 0 & K_{13} \\ 0 & K_{22} & K_{23} \\ K_{13}^T & K_{23}^T & K_{33} \end{pmatrix}, \tag{8}$$

where the subscripts 1, 2, 3 correspond to nodes in the interior of Ω^h, in the exterior, and on the boundary, respectively. We split the matrix K_{33} as follows:

$$K_{33} = K_{33}^{(1)} + K_{33}^{(2)}. \tag{9}$$

Here $K_{33}^{(1)}$ is constructed from the contributions of Ω^h to the integrals defining the elements of K_{33}, and $K_{33}^{(2)} = K_{33} - K_{33}^{(1)}$ contains the corresponding contributions from the complement $R - \Omega^h$.

The finite element discretization of the Neumann problem (4), (5) leads to a symmetric, positive semidefinite system of the form

$$\begin{pmatrix} K_{11} & K_{13} \\ K_{13}^T & K_{33}^{(1)} \end{pmatrix} \begin{pmatrix} \mathbf{x}_1 \\ \mathbf{x}_3 \end{pmatrix} = \begin{pmatrix} \mathbf{b}_1 \\ \mathbf{b}_3 \end{pmatrix}. \tag{10}$$

We wish to solve this system using the preconditioned conjugate gradient method. As a preconditioner for

$$\begin{pmatrix} K_{11} & K_{13} \\ K_{13}^T & K_{33}^{(1)} \end{pmatrix}, \tag{11}$$

we first consider

$$\left[\begin{pmatrix} I & 0 & 0 \\ 0 & 0 & I \end{pmatrix} K^{\oplus} \begin{pmatrix} I & 0 \\ 0 & 0 \\ 0 & I \end{pmatrix} \right]^{-1}, \tag{12}$$

where $K^{\oplus}$ denotes the Moore–Penrose pseudo-inverse of K.

LEMMA 1. *The matrix* (12) *exists, i.e.,*

$$\begin{pmatrix} I & 0 & 0 \\ 0 & 0 & I \end{pmatrix} K^{\oplus} \begin{pmatrix} I & 0 \\ 0 & 0 \\ 0 & I \end{pmatrix} \tag{13}$$

is invertible.

Proof. Let

$$\begin{pmatrix} \mathbf{x}_1 \\ \mathbf{x}_3 \end{pmatrix} \tag{14}$$

be a null vector of the matrix (13). Then we have

$$\begin{pmatrix} \mathbf{x}_1 \\ \mathbf{0} \\ \mathbf{x}_3 \end{pmatrix}^T K^{\oplus} \begin{pmatrix} \mathbf{x}_1 \\ \mathbf{0} \\ \mathbf{x}_3 \end{pmatrix} = \mathbf{0}. \tag{15}$$

Since $K^{\oplus}$ is a symmetric, positive semidefinite matrix, the vector

$$\begin{pmatrix} \mathbf{x}_1 \\ \mathbf{0} \\ \mathbf{x}_3 \end{pmatrix} \tag{16}$$

must then be an element of the kernel of $K^{\oplus}$. The kernel of $K^{\oplus}$ is the orthogonal complement of the range of K. Since K is symmetric, this implies

$$\ker(K^{\oplus}) = \ker(K) = \operatorname{span} \begin{pmatrix} 1 \\ \vdots \\ 1 \end{pmatrix}. \tag{17}$$

Therefore $\mathbf{x}_1$ and $\mathbf{x}_3$ must be zero. □

THEOREM 1. *Systems* (11) *and* (12) *are spectrally equivalent*, i.e., *the quotient of the quadratic forms associated with* (11) *and* (12) *is bounded, on the orthogonal complement of the kernel of* (11), *from below by* $\Lambda_0 > 0$ *and from above by* Λ_1, *with constants* Λ_0 *and* Λ_1 *independent of* h.

For a general proof of this theorem, see [6]. An outline of the idea of the proof can also be found in [1, § 4].

The convergence of the preconditioned conjugate gradient method depends on

$$\kappa := \frac{\Lambda_1}{\Lambda_0}. \tag{18}$$

The number of iterations needed to achieve a prescribed error reduction in a suitably chosen norm is proportional to $\sqrt{\kappa}$; see [3, p. 296].

Let $(\hat{\tau}_\nu)_{\nu=1,\cdots,n}$ be the triangulation of R obtained from $(\tau_\nu)_{\nu=1,\cdots,n}$ by moving the nodes (x_{ij}, y_{ij}) of the perturbed grid Γ back to their original positions $(\hat{x}_i, \hat{y}_j)$, and let $\hat{K}$ be the stiffness matrix based on this triangulation. $\hat{K}$ represents a five-point difference operator, and can be inverted by a direct fast Poisson solver if the mesh spacing in the grid $\hat{\Gamma}$ is uniform in at least one coordinate direction. For example, if the meshwidths in both coordinate directions are uniform and equal, then $\hat{K}$ represents the standard five-point difference operator

$$\begin{array}{ccc} & -1 & \\ -1 & 4 & -1. \\ & -1 & \end{array} \tag{19}$$

K also represents a difference operator, but near $\partial\Omega$, nine-point stencils may occur. Even if the grid $\hat{\Gamma}$ is uniform, this difference operator usually does not have constant coefficients, because of the irregular triangles near $\partial\Omega$. Therefore K cannot be inverted using a direct fast Poisson solver. In short, $\hat{K}$ is simpler than K.

We therefore replace K by $\hat{K}$ in (12). This increases the condition number κ by at most the factor

$$\operatorname{cond}[(\hat{K}^{\oplus})^{1/2} K (\hat{K}^{\oplus})^{1/2}], \tag{20}$$

where $\operatorname{cond}[\cdots]$ denotes the spectral condition number.

We will now estimate $\operatorname{cond}[(\hat{K}^{\oplus})^{1/2} K (\hat{K}^{\oplus})^{1/2}]$. Let τ be one of the triangles τ_ν, and let $\hat{\tau}$ be the corresponding triangle $\hat{\tau}_\nu$. Let ψ_τ be an affine mapping from $\hat{\tau}$ onto τ. There are several such affine mappings. To specify our choice, we require that ψ_τ maps any vertex $(\hat{x}_i, \hat{y}_j)$ of $\hat{\tau}$ onto the corresponding vertex (x_{ij}, y_{ij}) of τ.

THEOREM 2.

$$\operatorname{cond}[(\hat{K}^{\oplus})^{1/2} K (\hat{K}^{\oplus})^{1/2}] \leqq \max_{\tau=\tau_1,\cdots,\tau_n} \operatorname{cond}[(D\psi_\tau)^T (D\psi_\tau)], \tag{21}$$

where $D\psi_\tau$ *denotes the Jacobian of* ψ_τ.

Proof. Let ϕ denote a function belonging to the finite element space associated with the triangulation $(\tau_\nu)_{\nu=1,\cdots,n}$. That is, let ϕ be a continuous function on R which is linear on each of the triangles τ_ν. Let $\hat{\phi}$ denote the corresponding function in the finite element space associated with the triangulation $(\hat{\tau}_\nu)_{\nu=1,\cdots,n}$. That is, $\hat{\phi}$ is continuous on R, linear on each of the triangles $\hat{\tau}_\nu$, and $\hat{\phi}(\hat{x}_i, \hat{y}_j) = \phi(x_{ij}, y_{ij})$ for all pairs (i, j). Define

$$q(\phi) := \frac{\int_R |\nabla \phi|^2 \, d\mathbf{x}}{\int_R |\nabla \hat{\phi}|^2 \, d\mathbf{x}}. \tag{22}$$

Then

$$\text{cond}\,[(\hat{K}^{\oplus})^{1/2}K(\hat{K}^{\oplus})^{1/2}]=\frac{\max_{\phi} q(\phi)}{\min_{\phi} q(\phi)}, \tag{23}$$

where the maximum and minimum are taken over all nonzero ϕ. For $\nu=1,\cdots,n$, define

$$q_{\nu}(\phi):=\frac{\int_{\tau_{\nu}}|\nabla\phi|^2\,d\mathbf{x}}{\int_{\hat{\tau}_{\nu}}|\nabla\hat{\phi}|^2\,d\mathbf{x}}. \tag{24}$$

Then

$$\frac{\max_{\phi} q(\phi)}{\min_{\phi} q(\phi)}\leqq\frac{\max_{\phi,\nu} q_{\nu}(\phi)}{\min_{\phi,\nu} q_{\nu}(\phi)}, \tag{25}$$

where the maximum and minimum on the right-hand side of (25) is taken over all nonzero ϕ and all $\nu\in\{1,\cdots,n\}$. We note that (25) is not sharp.

To prove the assertion, we must now estimate the quotients $q_{\nu}(\phi)$ from above and below. Change of variables gives

$$\int_{\tau}|\nabla\phi|^2\,d\mathbf{x}=\int_{\hat{\tau}}(\nabla\hat{\phi})^T(D\psi_{\tau})^{-1}(D\psi_{\tau})^{-T}(\nabla\hat{\phi})|\det(D\psi_{\tau})|\,d\mathbf{x}. \tag{26}$$

This shows that $q_{\nu}(\phi)$ lies in the interval

$$[\lambda_{\min}((D\psi_{\tau})^{-1}(D\psi_{\tau})^{-T})|\det(D\psi_{\tau})|,\ \lambda_{\max}((D\psi_{\tau})^{-1}(D\psi_{\tau})^{-T})|\det(D\psi_{\tau})|], \tag{27}$$

where $\lambda_{\min}(\cdots)$ denotes the smaller eigenvalue and $\lambda_{\max}(\cdots)$ the larger one. Define

$$e:=\lambda_{\min}((D\psi_{\tau})^{-1}(D\psi_{\tau})^{-T}), \tag{28}$$

$$E:=\lambda_{\max}((D\psi_{\tau})^{-1}(D\psi_{\tau})^{-T}). \tag{29}$$

Then

$$|\det(D\psi_{\tau})|=\sqrt{\det((D\psi_{\tau})^T(D\psi_{\tau}))}=\frac{1}{\sqrt{\det((D\psi_{\tau})^{-1}(D\psi_{\tau})^{-T})}}=\frac{1}{\sqrt{eE}}, \tag{30}$$

and therefore

$$\begin{aligned}\lambda_{\min}((D\psi_{\tau})^{-1}(D\psi_{\tau})^{-T})|\det(D\psi_{\tau})|&=e\cdot\frac{1}{\sqrt{eE}}=\sqrt{\frac{e}{E}}\\&=\sqrt{\frac{1}{\text{cond}\,[(D\psi_{\tau})^{-1}(D\psi_{\tau})^{-T}]}}\\&=\sqrt{\frac{1}{\text{cond}\,[(D\psi_{\tau})^{T}(D\psi_{\tau})]}}.\end{aligned} \tag{31}$$

Similarly,

$$\lambda_{\max}((D\psi_{\tau})^{-1}(D\psi_{\tau})^{-T})|\det(D\psi_{\tau})|=\sqrt{\frac{E}{e}}=\sqrt{\text{cond}\,[(D\psi_{\tau})^{T}(D\psi_{\tau})]}. \tag{32}$$

The assertion now follows. □

3. The triangulation algorithm. We first assume that $\partial\Omega\in C^2$. Modifications for domains with corners will be discussed later.

We define a function

$$\hat{\phi}:\hat{\Gamma}\to\{-1,0,1\} \tag{33}$$

by the following algorithm.

For $\hat{\mathbf{x}} \in \hat{\Gamma}$, define first $\hat{\phi}(\hat{\mathbf{x}}) = 1$ if $\hat{\mathbf{x}} \in \Omega$, and $\hat{\phi}(\hat{\mathbf{x}}) = -1$ if $\hat{\mathbf{x}} \notin \Omega$.
Then modify the values $\hat{\phi}(\hat{\mathbf{x}})$ in the following way.
For $i = 0, \cdots, I-1$:
For $j = 0, \cdots, J-1$:
If $\hat{\phi}(ih, jh) \cdot \hat{\phi}((i+1)h, jh) = -1$: Determine $x \in [ih, (i+1)h]$ with $(x, jh) \in \partial\Omega$; if $x \geqq (i+\frac{1}{2})h$, set $\hat{\phi}((i+1)h, jh) = 0$; otherwise set $\hat{\phi}(ih, jh) = 0$.
If $\hat{\phi}(ih, jh) \cdot \hat{\phi}(ih, (j+1)h) = -1$: Determine $y \in [jh, (j+1)h]$ with $(ih, y) \in \partial\Omega$; if $y \geqq (j+\frac{1}{2})h$, set $\hat{\phi}(ih, (j+1)h) = 0$; otherwise set $\hat{\phi}(ih, jh) = 0$.

Note that the triangulation depends on the order in which we inspect the points (ih, jh). Instead of the columnwise lexicographic ordering that we have used here, row-wise lexicographic ordering could be used, and would lead to a possibly slightly different, but similar triangulation.

We define

$$\hat{I} := \{\hat{\mathbf{x}} \in \hat{\Gamma} \colon \hat{\phi}(\hat{\mathbf{x}}) = 1\}, \tag{34}$$

$$\hat{B} := \{\hat{\mathbf{x}} \in \hat{\Gamma} \colon \hat{\phi}(\hat{\mathbf{x}}) = 0\}, \tag{35}$$

$$\hat{E} := \{\hat{\mathbf{x}} \in \hat{\Gamma} \colon \hat{\phi}(\hat{\mathbf{x}}) = -1\}. \tag{36}$$

Points in $\hat{I}$, $\hat{B}$, and $\hat{E}$ are called interior, boundary, and exterior points, respectively. The set of points in Γ that correspond to the boundary points in $\hat{\Gamma}$ is denoted by B. Thus

$$\Gamma = \hat{I} \cup B \cup \hat{E}. \tag{37}$$

By construction, the set of boundary points $\hat{B}$ has no holes, in the following sense.

LEMMA 2. *If $\hat{\mathbf{x}}^{(1)}$ and $\hat{\mathbf{x}}^{(2)}$ are neighbor points in $\hat{\Gamma}$, i.e., $\hat{\mathbf{x}}^{(1)} = (\hat{x}_i, \hat{y}_i)$ and $\hat{\mathbf{x}}^{(2)} = (\hat{x}_{i\pm1}, \hat{y}_j)$ or $\hat{\mathbf{x}}^{(2)} = (\hat{x}_i, \hat{y}_{j\pm1})$, then $\hat{\phi}(\hat{\mathbf{x}}^{(1)}) \cdot \hat{\phi}(\hat{\mathbf{x}}^{(2)}) \neq -1$.*

Let $0 \leqq i \leqq I-1$ and $0 \leqq j \leqq J-1$, and let Q be the quadrilateral with vertices $\mathbf{x}_{ij}$, $\mathbf{x}_{i+1,j}$, $\mathbf{x}_{i,j+1}$, and $\mathbf{x}_{i+1,j+1}$. Q is cut into two triangles along one of its diagonals, and a decision is made for each of them if it belongs to the approximation Ω^h of Ω or to $R - \Omega^h$.

To decide how to cut Q, we need a way of measuring the degeneracy of the resulting triangles. We assign a number μ to a pair (Q, d), where d is a diagonal of Q, as follows. Cutting Q along d gives two triangles $\tau^{(1)}$ and $\tau^{(2)}$. Let $\hat{\tau}^{(1)}$ and $\hat{\tau}^{(2)}$ be the corresponding regular triangles with vertices in $\hat{\Gamma}$. Let $\psi^{(k)}$ be an affine mapping from $\hat{\tau}^{(k)}$ onto $\tau^{(k)}$, $k = 1, 2$. There are several such affine mappings, and we specify our choice in the way explained before Theorem 2. We then define

$$\mu := \min_{k=1,2} \frac{\det D\psi^{(k)}}{\lambda_{\max}((D\psi^{(k)})^T (D\psi^{(k)}))}. \tag{38}$$

As before, $\lambda_{\max}(\cdot)$ denotes the larger of the two eigenvalues. The two values of μ, corresponding to the two diagonals of Q, are used below to decide how Q is to be divided. μ is negative if and only if Q is not convex and d lies outside Q. Thus, at least one of the two values of μ associated with the two diagonals of Q will always be positive. The larger μ is, the less degenerate is the configuration resulting from cutting Q along d.

The triangulation algorithm of Proskurowski and Widlund [4] is quite different from ours, but also uses a "degeneracy measure," namely

$$\frac{1}{\text{length of } d}. \tag{39}$$

In many cases, this criterion is roughly equivalent to ours. However, suppose that the vertices of Q are

$$((i+\tfrac{1}{2})h, jh), \quad ((i+1)h, (j+\tfrac{1}{2})h), \quad ((i+\tfrac{3}{2})h, (j+1)h), \quad (ih, (j+\tfrac{3}{2})h). \tag{40}$$

Q has a 180 degree angle. Criterion (39) does not detect the difference between the two possible ways of cutting Q, and this can result in a triangle of zero area.

Definition (38) is motivated by Theorem 2, together with the observation that

$$\mu = \min_{k=1,2} \frac{1}{\operatorname{cond}[(D\psi^{(k)})^T(D\psi^{(k)})]} \quad \text{if } \mu > 0. \tag{41}$$

We shall now describe how μ is used to decide along which diagonal to cut the quadrilateral cells Q of the grid Γ, and which of the resulting triangles to include in Ω^h. Let $\mathbf{x}^{(m)}$, $m = 1, 2, 3, 4$ be the vertices of Q. Let n_I be the number of points in

$$\hat{I} \cap \{\mathbf{x}^{(1)}, \mathbf{x}^{(2)}, \mathbf{x}^{(3)}, \mathbf{x}^{(4)}\}, \tag{42}$$

and let n_B and n_E be defined analogously.

Case 1. $n_E \geqq 2$. Then $n_I = 0$. If $n_E = 4$, Q is a rectangle and is cut along the diagonal joining the left upper and the right lower vertex. In all other cases, we maximize μ. Both triangles belong to $R - \Omega^h$.

Case 2. $n_I \geqq 2$. This case is analogous to Case 1.

Case 3. $n_E = 1$, $n_I = 1$. Using Lemma 2, it is easy to see that Q is convex in this case. We cut along the diagonal joining the two vertices of Q belonging to the set of boundary points B in Γ.

Case 4. $n_E = 1$, $n_I = 0$, $n_B = 3$. We attempt to cut such that all three vertices of one of the two resulting triangles lie in B. If the resulting configuration is nondegenerate, and if the centroid of the triangle with three vertices in B lies in Ω, we include this triangle in Ω^h and the remaining one in $R - \Omega^h$. In all other cases, we proceed as in Case 1.

Case 5. $n_I = 1$, $n_E = 0$, $n_B = 3$. This case is analogous to Case 4.

Case 6. $n_E = n_I = 0$, $n_B = 4$. We maximize μ. Each resulting triangle is included in Ω^h if and only if its centroid belongs to Ω.

This concludes the description of our algorithm for smooth domains. The triangulations are guaranteed to be nondegenerate, and $\partial\Omega^h$ is close to $\partial\Omega$, as shown by the following theorem.

THEOREM 3. *Let τ be one of the triangles generated by our algorithm, and let ψ_τ be as in Theorem 2. Then*

$$\operatorname{cond}[(D\psi_\tau)^T(D\psi_\tau)] \leqq \gamma := (3+\sqrt{8})^2 \approx 34. \tag{43}$$

This estimate is sharp. If $\partial\Omega \in C^2$, then

$$\operatorname{dist}(\partial\Omega, \partial\Omega^h) \leqq O(h^2). \tag{44}$$

Proof. Estimate (43) follows from a detailed but straightforward examination of the six cases.

To prove (44), observe first that every node $\mathbf{x}$ on $\partial\Omega^h$ belongs to the set B of boundary nodes in Γ, and therefore to $\partial\Omega$. To see that $\mathbf{x} \in B$, note that $\mathbf{x}$ must belong to some interior triangle, and therefore $\mathbf{x} \notin \hat{E}$. Similarly, we conclude $\mathbf{x} \notin \hat{I}$, and thus $\mathbf{x} \in B$. (We remark that the converse is not necessarily true: There may be nodes in B that do not belong to $\partial\Omega^h$, if there are several very close intersections of a grid line with $\partial\Omega$.)

The boundary $\partial\Omega^h$ thus consists of straight-line segments of length $O(h)$ joining points on $\partial\Omega$. For $\partial\Omega \in C^2$, this implies (44). $\square$

From Theorems 2 and 3, it follows that the condition number of $(\hat{K}^{\oplus})^{1/2}K(\hat{K}^{\oplus})^{1/2}$ is bounded independently of Ω of h. (We recall, however, that the estimate of Theorem 2, unlike that of Theorem 3, is not sharp, since (25) is not sharp.) In combination with Theorem 1, this result shows that the number of iterations required to achieve a prescribed accuracy with the domain imbedding algorithm described in § 2, using our triangulation algorithm, is bounded independently of the meshwidth. Numerical results confirming this can be found in [1, Table 1].

We have made no specific assumptions on how the region is represented on the computer. We only assume that a subroutine is available to decide if a given point $\mathbf{x} \in R$ lies in Ω or not. If this decision can be made in $O(1)$ operations, the total number of operations required by our algorithm is $O(N^2 + n_B \log(1/\varepsilon))$, where $\varepsilon > 0$ is the error tolerance for determining the intersections of the boundary with grid lines. If the boundary is given in parametric form, our algorithm can be modified such that it requires only $O(n_B \log(1/\varepsilon))$ operations, by restricting the search for intersections of $\partial\Omega$ with grid lines to a strip along $\partial\Omega$, of width comparable to the meshwidth of $\hat{\Gamma}$.

The algorithm described so far frequently cuts off corners of $\partial\Omega$. In our code we have implemented the following modification, which leads to satisfactory triangulations for many domains with corners.

In addition to the subroutine defining the domain Ω, the user specifies a finite set P of points in the rectangle R, typically the corner points of $\partial\Omega$. The modified algorithm will attempt to construct the triangulation in such a way that all points in P become vertices of $\partial\Omega^h$. We assume that the grid $\hat{\Gamma}$ is sufficiently fine, in the following sense. If $\hat{\mathbf{x}}^{(1)} \in P$ and $\hat{\mathbf{x}}^{(2)} \in P$, and if $(\hat{x}_i, \hat{y}_j) \in \hat{\Gamma}$,

$$\hat{\mathbf{x}}^{(1)} \in \left[\frac{\hat{x}_{i-1}+\hat{x}_i}{2}, \frac{\hat{x}_{i+1}+\hat{x}_i}{2}\right] \times \left[\frac{\hat{y}_{j-1}+\hat{y}_j}{2}, \frac{\hat{y}_{j+1}+\hat{y}_j}{2}\right], \tag{45}$$

then

$$\hat{\mathbf{x}}^{(2)} \notin \left[\frac{\hat{x}_{i-2}+\hat{x}_{i-1}}{2}, \frac{\hat{x}_{i+2}+\hat{x}_{i+1}}{2}\right] \times \left[\frac{\hat{y}_{j-2}+\hat{y}_{j-1}}{2}, \frac{\hat{y}_{j+2}+\hat{y}_{j+1}}{2}\right]. \tag{46}$$

The initialization of the function $\hat{\phi}$ is modified in the following way. If $\hat{\mathbf{x}} = (\hat{x}_i, \hat{y}_j)$ is a point in $\hat{\Gamma}$, and if there is a point in P contained in the rectangle

$$\left[\frac{\hat{x}_{i-1}+\hat{x}_i}{2}, \frac{\hat{x}_{i+1}+\hat{x}_i}{2}\right] \times \left[\frac{\hat{y}_{j-1}+\hat{y}_j}{2}, \frac{\hat{y}_{j+1}+\hat{y}_j}{2}\right], \tag{47}$$

then we initially set $\hat{\phi}(\hat{\mathbf{x}}) = 0$; otherwise we set $\hat{\phi}(\hat{\mathbf{x}}) = 1$ for $\hat{\mathbf{x}} \in \Omega$ and $\hat{\phi}(\hat{\mathbf{x}}) = -1$ for $\hat{\mathbf{x}} \notin \Omega$.

With this modification, the triangulations generated are still nondegenerate uniformly in h and Ω. The constant in (43) now becomes

$$\gamma = (15+\sqrt{221})^2/4 \approx 223. \tag{48}$$

For domains with corners, estimates (44) (with some domain independent constant γ) and (43) cannot hold at the same time, no matter how the definition of the function $\hat{\phi}$ is modified. The reason is that $\partial\Omega$ might have a corner with an arbitrarily small angle. Obviously, such a corner will require either the degeneracy of some triangles, or to be cut off, with the consequence that (44) no longer holds.

4. Figures. Figure 1 shows the regular grid $\hat{\Gamma}$. Figure 2 shows the perturbed grid Γ for the case of a disk Ω imbedded in a square. Figures 3–5 show the triangulations of a domain Ω, its complement, and the triangulation of the entire rectangle R, which is a square here.

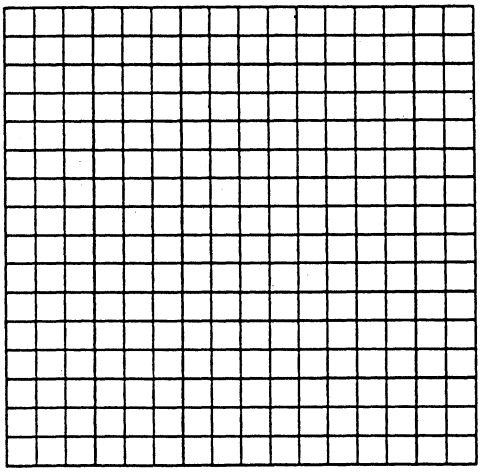

FIG. 1. *The regular grid* $\hat{\Gamma}$.

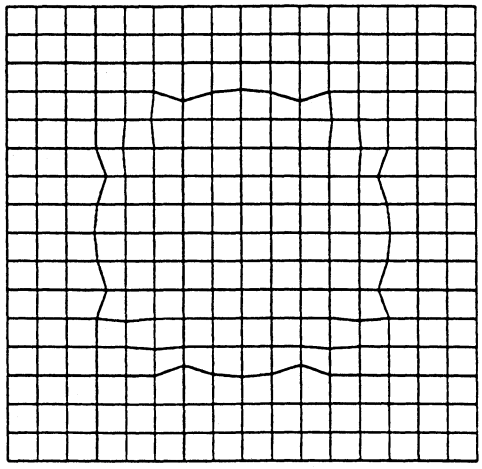

FIG. 2. *The perturbed grid* Γ.

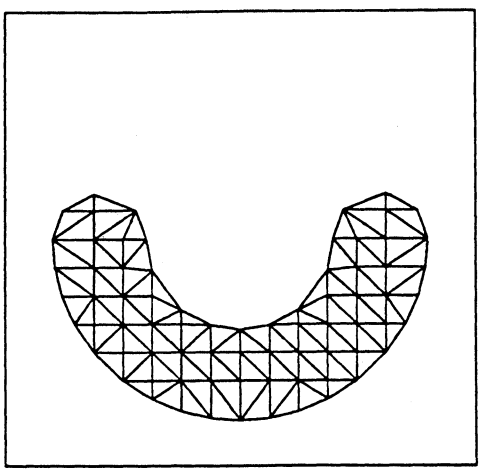

FIG. 3. *Triangulation of* Ω.

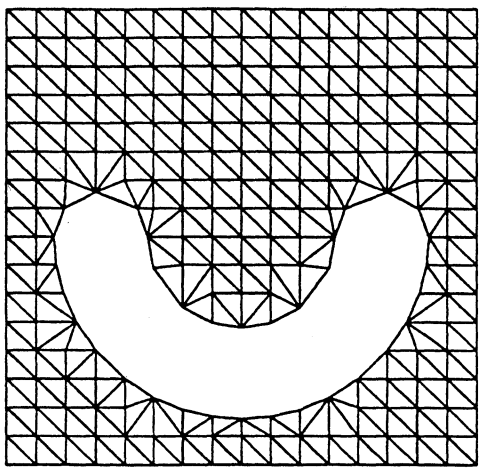

FIG. 4. *Triangulation of the complement of* Ω.

5. Summarizing discussion. In this section, we will briefly discuss the role of domain imbedding in solving elliptic boundary value problems, and the significance of the work presented in this paper.

Domain imbedding methods have the advantage of simplicity. This is illustrated by the method described in § 2. All that is required to implement this method is the formulation of the finite element problem, a fast solver on the rectangle R, and few additional lines of code to implement the conjugate gradient iteration. The formulation of the finite element problem requires a triangulation of the kind generated by the algorithm presented in this paper, and the generation of stiffness and mass matrices. The latter can be done locally: All that is needed is the computation of stiffness and mass submatrices for each triangle, again requiring only few lines of code. Our triangulation algorithm thus forms the major part of a solver for Neumann problems for the Poisson equation on general bounded domains in two dimensions. Domain imbedding can also be applied to other elliptic boundary value problems, for example,

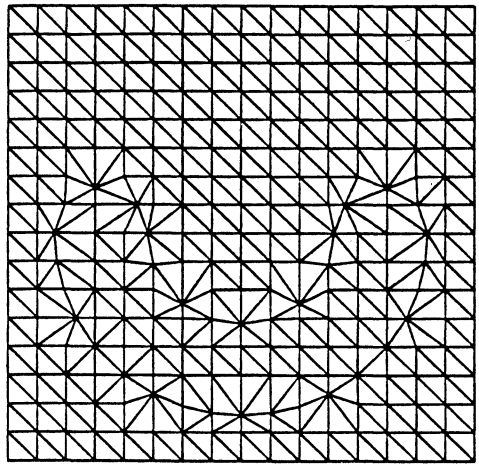

FIG. 5. *Triangulation of* Ω *and its complement.*

Dirichlet problems, and problems for more general second order elliptic equations. The triangulations generated by our algorithm can also be used in these cases. We refer to [1] for a survey and study of elliptic solvers based on domain imbedding.

However, domain imbedding methods have several limitations. Although they are efficient in comparison to most elliptic solvers, good multigrid algorithms are usually faster by at least a factor of 2 or 3, and often more; compare, e.g., the numerical experiments of [1] to those of [5, p. 147]. However, Dendy has suggested the use of his black box multigrid algorithm for domain imbedding (see [2, p. 380]). This approach has a weaker theoretical foundation than the one described in § 2, but it appears to lead to a considerably more efficient method; compare the numerical experiments on page 381 of [2]. We note that our triangulation algorithm could also be used in combination with Dendy's algorithm.

A severe principal limitation of domain imbedding methods lies in the need for almost uniform grids such as the ones constructed by our algorithm. However, if local grid refinement is needed, domain imbedding may still be a useful technique on the coarsest level of a multigrid algorithm, using a hierarchy of grids with local refinement on the fine levels. This type of elliptic solver is particularly attractive when complete coarsening of the grid is either inconvenient because of geometric complications, or undesirable, as might be the case on parallel computers.

Acknowledgment. I am grateful to Olof Widlund for many helpful discussions.

REFERENCES

[1] C. BÖRGERS AND O. B. WIDLUND, *On finite element domain imbedding methods*, SIAM J. Numer. Anal., 27 (1990), pp. 962–977.

[2] J. E. DENDY, *Black box multigrid*, J. Comput. Phys., 48 (1982), pp. 366–386.

[3] D. G. LUENBERGER, *Optimization by Vector Space Methods*, John Wiley, New York, 1969.

[4] W. PROSKUROWSKI AND O. B. WIDLUND, *A finite element capacitance matrix method for the Neumann problem for Laplace's equation*, SIAM J. Sci. Statist. Comput., 1 (1980), pp. 410–425.

[5] K. STÜBEN AND U. TROTTENBERG, *Multigrid methods: fundamental algorithms, model problem analysis and applications*, in Lecture Notes in Math. 960, Springer-Verlag, Berlin, New York, 1982, pp. 1–176.

[6] O. B. WIDLUND, *An extension theorem for finite element spaces with three applications*, in Proc. Second GAMM Seminar, Kiel, FRG, January 1986, Notes Numer. Fluid Mech. 16, W. Hackbusch and K. Witsch, eds., F. Vieweg, Braunschweig, Wiesbaden, 1987.